OXFORD
SOT | Society of Toxicology
www.toxsci.oxfordjournals.org
ToxSci 20 Years

TOXICOLOGICAL SCIENCES, 163(1), 2018, 13–25

doi: 10.1093/toxsci/kfx291
Advance Access Publication Date: January 2, 2018
Research Article

Aberrant Epigenetic Gene Regulation in GABAergic Interneuron Subpopulations in the Hippocampal Dentate Gyrus of Mouse Offspring Following Developmental Exposure to Hexachlorophene

Yousuke Watanabe,[*,†] Hajime Abe,[*] Kota Nakajima,[*,†] Maky Ideta-Otsuka,[‡] Katsuhide Igarashi,[‡] Gye-Hyeong Woo,[§] Toshinori Yoshida,[*] and Makoto Shibutani[*,¶,1]

[*]Laboratory of Veterinary Pathology, Division of Animal Life Science, Institute of Agriculture, Tokyo University of Agriculture and Technology, Fuchu-shi, Tokyo 183-8509, Japan; [†]Pathogenetic Veterinary Science, United Graduate School of Veterinary Sciences, Gifu University, Gifu-shi, Gifu 501-1193, Japan; [‡]Life Science Tokyo Advanced Research Center (L-StaR), Hoshi University School of Pharmacy and Pharmaceutical Sciences, Shinagawa-ku, Tokyo 142-5801, Japan; [§]Laboratory of Histopathology, Department of Clinical Laboratory Science, Semyung University, Jecheon-si, Chungbuk 27136, Republic of Korea; and [¶]Institute of Global Innovation Research, Tokyo University of Agriculture and Technology, Fuchu-shi, Tokyo 183-8509, Japan

[1]To whom correspondence should be addressed at Laboratory of Veterinary Pathology, Division of Animal Life Science, Institute of Agriculture, Tokyo University of Agriculture and Technology, 3-5-8 Saiwai-cho, Fuchu-shi, Tokyo 183-8509, Japan. Tel/Fax: +81-42-367-5771. E-mail: mshibuta@cc.tuat.ac.jp.

ABSTRACT

Maternal hexachlorophene (HCP) exposure causes transient disruption of hippocampal neurogenesis in mouse offspring. We examined epigenetically hypermethylated and downregulated genes related to this HCP-induced disrupted neurogenesis. Mated female mice were dietary exposed to 0 or 100 ppm HCP from gestational day 6 to postnatal day (PND) 21 on weaning. The hippocampal dentate gyrus of male offspring was subjected to methyl-capture sequencing and real-time reverse transcription-polymerase chain reaction analyses on PND 21. Validation analyses on methylation identified three genes, *Dlx4*, *Dmrt1*, and *Plcb4*, showing promoter-region hypermethylation. Immunohistochemically, $DLX4^+$, $DMRT1^+$, and $PLCB4^+$ cells in the dentate hilus co-expressed GAD67, a γ-aminobutyric acid (GABA)ergic neuron marker. HCP decreased all of three subpopulations as well as $GAD67^+$ cells on PND 21. $PLCB4^+$ cells also co-expressed the metabotropic glutamate receptor, GRM1. HCP also decreased transcript level of synaptic plasticity-related genes in the dentate gyrus and immunoreactive granule cells for synaptic plasticity-related ARC. On PND 77, all immunohistochemical cellular density changes were reversed, whereas the transcript expression of the synaptic plasticity-related genes fluctuated. Thus, HCP-exposed offspring transiently reduced the number of GABAergic interneurons. Among them, subpopulations expressing DLX4, DMRT1, or PLCB4 were transiently reduced in number through an epigenetic mechanism. Considering the role of the *Dlx* gene family in GABAergic interneuron migration and differentiation, the decreased number of $DLX4^+$ cells may be responsible for reducing those GABAergic interneurons regulating neurogenesis. The effect on granule cell synaptic plasticity was sustained until the adult stage, and reduced GABAergic interneurons active in GRM1–PLCB4 signaling may be responsible for the suppression on weaning.

Key words: epigenetic gene regulation; GABAergic interneuron; hexachlorophene; hippocampal dentate gyrus; hypermethylation; neurogenesis.

The hippocampal dentate gyrus of the mammalian brain is crucial for higher brain functions, such as learning and memory that are correlated with adult hippocampal neurogenesis and activity-dependent synaptic plasticity (Vivar *et al.*, 2013). During postnatal life, adult neurogenesis continues in the subgranular zone (SGZ) of the dentate gyrus (Zhao *et al.*, 2008). The γ-aminobutyric acid (GABA)ergic interneurons in the hilus of the dentate gyrus innervate granule cell lineage populations to control neurogenesis in the SGZ (Masiulis *et al.*, 2011). In addition to GABAergic neuronal inputs, various neurons outside the SGZ create synaptic connections with neurons in the dentate gyrus, such as cholinergic neurons and glutamatergic neurons (Fonnum *et al.*, 1979; Zhu *et al.*, 2008). Both cholinergic and glutamatergic inputs to the SGZ are important for maintaining proper proliferation and differentiation of granule cell lineages (Cameron *et al.*, 1995; Zhu *et al.*, 2008).

Hexachlorophene (HCP), used as an antimicrobial agent in soaps, liquid detergents, and cosmetics during the 1960s, had been widely used in agriculture as a plant fungicide and pesticide (Kennedy *et al.*, 1976). HCP, now established as a typical neurotoxin, induces myelin vacuolation corresponding to the splitting of the intraperiod line of the myelin sheath in the cerebral white matter of rodents (Lampert *et al.*, 1973). In chronically exposed rats, segmental demyelination and remyelination progress, and a few fibers undergo axonal degeneration (Maxwell and Le Quesne, 1979). Experimentally, HCP can be transferred into offspring through placenta and milk (Kennedy *et al.*, 1977). In our previous study, developmental exposure of mice to HCP also induced myelin vacuolation in the brains of the offspring (Kato *et al.*, 2016).

Because adult neurogenesis includes all processes from neuronal production to maturation, it has been thought that hippocampal neurogenesis is a sensitive target of both developmental and adult neurotoxicants. In particular, chemical toxicity could affect self-renewal of stem cells, proliferation and migration of progenitor cells, neuritogenesis, synaptogenesis, and myelinogenesis. It is possible that developmental neurotoxicant exposure causes abnormalities in the formation of the dentate gyrus and the regulatory system of adult neurogenesis to result in alterations in neurogenesis. We have recently shown that developmental exposure to glycidol, which targets axon terminals, impairs late-stage differentiation of the neurogenesis process involving density changes of interneuron subpopulations in the dentate hilus of rat offspring (Akane *et al.*, 2013a). Furthermore, developmental exposure to HCP impairs intermediate-stage progenitor cells in the SGZ in rat or mouse offspring, probably by reducing nerve conduction velocity of regulatory neurons of neurogenesis (Itahashi *et al.*, 2015; Kato *et al.*, 2016). In our mouse HCP developmental exposure study, however, we observed no fluctuations in the density of GABAergic interneuron subpopulations in the dentate hilus, whereas transcript downregulations of cholinergic receptors and glutamate receptors were observed in the dentate gyrus, likely related to the disruption of hippocampal neurogenesis (Supplementary Figs. 1–3; Kato *et al.*, 2016).

Recent studies indicate that various epigenetic mechanisms, including DNA methylation, are involved in regulating different aspects of adult neurogenesis (Sun *et al.*, 2011). The understanding of DNA methylation as a long-lasting cellular memory necessary to maintain a cellular phenotype has recently been challenged by discoveries of its dynamic nature (Covic *et al.*, 2010). This relationship is particularly common in CpG sites at promoter regions, where DNA methylation may directly interfere with transcription factor binding to DNA or indirectly suppress transcription through methylated DNA-binding proteins that recruit histone deacetylases, leading to chromatin condensation and subsequent gene silencing (Jones *et al.*, 1998). Although the results of epigenetic changes on neurogenesis have remained unexplored, environmentally induced disruption of DNA methylation warrants further study (Ceccatelli *et al.*, 2013), given the clear importance of DNA methylation to neuronal development. In fact, exposure to stress (Mueller and Bale, 2008), toxicants (Kundakovic *et al.*, 2013), and maternal neglect (Weaver *et al.*, 2004) in early life has shown to disrupt epigenetic programming involving DNA methylation in the brain, with lasting consequences for brain gene expression and behavior.

The present study was performed to clarify the potential effects of maternal HCP exposure on epigenetic regulation in the development of the hippocampal dentate gyrus that may affect adult neurogenesis in mouse offspring. For this purpose, the hippocampal dentate gyrus of male offspring was first subjected to a search for genes with downregulated transcripts induced by promoter region hypermethylation. We then examined the reversibility of the methylation status, transcript levels, and cellular distribution of the corresponding proteins in the dentate gyrus.

MATERIALS AND METHODS

Chemicals and animals. HCP (purity: >99%) was purchased from MP Biomedicals, LLC (Santa Ana, California). Mated female Slc: ICR mice were purchased from Japan SLC Inc. (Hamamatsu, Japan) at gestational day (GD) 1 (appearance of vaginal plugs was designated GD 0) and individually housed with their offspring in plastic cages containing paper chip bedding until postnatal day (PND) 21. Animals were maintained in an air-conditioned animal room (temperature: 23 ± 2°C, relative humidity: 55% ± 15%) with a 12-h light/dark cycle and provided MF basal diet purchased from Oriental Yeast Co., Ltd. (Tokyo, Japan) mixed with HCP and tap water from GD 6 to PND 21. Beginning on PND 21, male and female offspring were separated and reared with three or four animals per cage and provided MF basal diet and tap water *ad libitum*.

Animal experiment. The animal experimental protocol and samples used were identical to that previously reported (Kato *et al.*, 2016), and exposure period and number of animals per group were in accordance with the OECD test guideline for the testing chemicals (Test No. 426: Developmental Neurotoxicity Study; OECD, 2007). In brief, mated female mice were randomly divided into three groups of 12 animals each and were treated with 0, 33, or 100 ppm HCP, which was mixed with their food, from GD 6 to day 21 after delivery, which was the day of weaning (Figure 1). On PND 3, the litters were randomly culled to preserve eight males per litter. If dams had fewer than eight male pups, female pups were added to maintain a total of eight pups per litter. Because neurogenesis is influenced by circulating

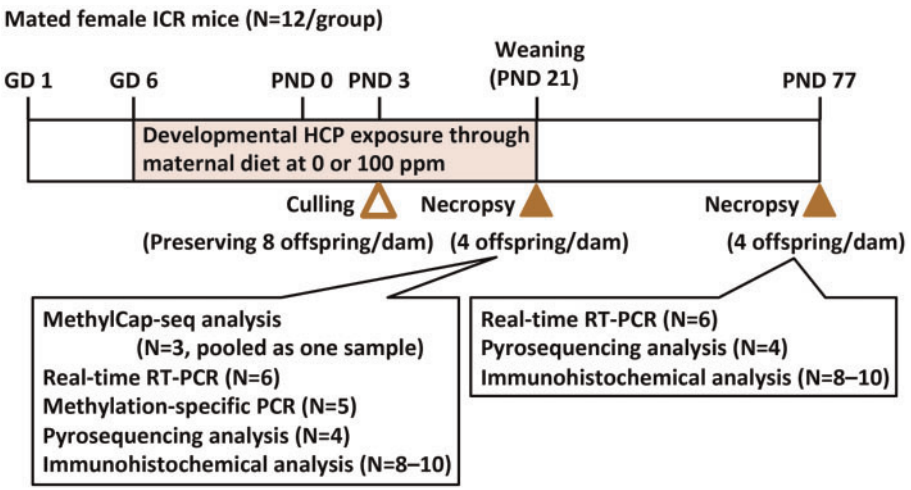

Figure 1. Experimental design for the developmental exposure study of hexachlorophene (HCP) using mated female mice. Eight offspring were preserved in each dam after culling on postnatal day (PND) 3, and offspring were subjected to molecular and immunohistochemical analyses in the hippocampal dentate gyrus. One offspring per dam was used in each analysis.

levels of steroid hormones during the estrous cycle (Pawluski *et al.*, 2009), only male offspring were used for all analyses in the present study. On PND 21, 10–11 male animals per group (one male offspring per dam) were randomly selected for use in brain immunohistochemistry assays and subjected to perfusion fixation through the left cardiac ventricle with cold 4% (w/v) paraformaldehyde (PFA) after deep anesthesia with CO_2/O_2. For perfusion, a Masterflex peristaltic pump (EW-7553-70/71; Cole-Parmer, Vernon Hills, Illinois) was used to apply a flow rate of 10 mL/min. On PND 77, 10–11 male offspring per group (one male offspring per dam) were also randomly selected for immunohistochemistry analysis and perfused with cold 4% PFA at a flow rate of 10 mL/min.

All procedures in this study were conducted in compliance with the Guidelines for Proper Conduct of Animal Experiments (Science Council of Japan, June 1, 2006) and according to the protocol approved by the Animal Care and Use Committee of Tokyo University of Agriculture and Technology. All efforts were made to minimize animal suffering.

DNA and RNA extraction. For DNA and RNA extraction, male offspring brains were removed under CO_2/O_2 anesthesia on PND 21 and PND 77, fixed with methacarn solution for 5 h at 4°C, and then dehydrated in ice-cold absolute ethanol overnight at 4°C, as described previously (Akane *et al.*, 2013b). A coronal brain slice obtained from a position at −2.2 mm from the bregma was prepared. Portions of the hippocampal dentate gyrus were collected using a biopsy punch (Φ1.0 mm; Kai Industries Co. Ltd., Seki, Japan) and stored in ethanol at −80°C until used for extraction.

For methylation analysis, genomic DNA and total RNA were extracted from tissue samples of the 0 ppm controls and the 100-ppm HCP-exposed group on PND 21 and PND 77 using an All-prep DNA/RNA mini kit (Qiagen, Hilden, Germany). As shown in Figure 1, extracted DNA was used for methyl-capture sequencing (MethylCap-seq) analysis ($n = 3$/group, pooled as one sample), quantitative methylation-specific PCR analysis ($n = 5$/group), and pyrosequencing assays ($n = 4$/group). Extracted total RNA was used for real-time RT-PCR analysis ($n = 6$/group).

MethylCap-seq analysis. MethylCap-seq analysis was performed in accordance with the manufacturers' provided protocols using pooled genomic DNA sample of the 0 ppm controls and the 100-ppm HCP-exposed group on PND 21. In brief, genomic DNA was fragmented using a Bioruptor UCD-250 sonicator (Cosmo Bio Co. Ltd., Tokyo, Japan), and methylated DNA was enriched with methyl-CpG-binding domain 2 (MBD2) protein using an EpiXplore™ Methylated DNA Enrichment kit (Clontech Laboratories, Inc., Mountain View, Canada). Subsequently, enriched methylated DNA was used to construct libraries for sequencing using a DNA NEB® Next ChIP-Seq Library Prep Master Mix Set for Illumina® (New England Biolabs, Inc., Ipswich, Massachussets). The libraries, one from 0 ppm controls and the other from 100-ppm HCP-exposed group, were sequenced using a Miseq Sequencing System (Illumina, Inc., San Diego, California), and then data analysis was performed using Strand NGS (next-generation sequencing) analysis software (Strand Genomics, Inc., San Francisco, California). The genomic regions showing hypermethylation of CpG sites in the promoter region up to 1000 bp upstream from the transcription start site of the genes were selected using an enriched region detection algorithm with the criterion that the enrichment factor (ratio of HCP-exposed sample read counts/control sample read counts) was greater than 5.

Transcript expression analysis of candidate genes. Real-time RT-PCR quantification of mRNA was performed for genes selected as being hypermethylated using the MethylCap-seq data analysis with the RNA samples isolated from the 0 ppm controls and the 100-ppm HCP-exposed group on PND 21. The genes showing transcript downregulation on PND 21 were also analyzed for expression on PND 77. First-strand complementary DNA was synthesized using SuperScript® III Reverse Transcriptase (Thermo Fisher Scientific, Waltham, Massachussets) in a total reaction mixture of 20 μl from 1.0 μg of total RNA. Analysis of the transcript levels for candidate genes listed in Table 1 was performed using the PCR primers designed with Primer Express software Ver. 3.0 (Supplementary Table 1; Thermo Fisher Scientific). Real-time RT-PCR with Power SYBR® Green PCR Master Mix (Thermo Fisher Scientific) was conducted using a StepOnePlus™ Real-time PCR System (Thermo Fisher Scientific). The relative

Table 1. Genes Downstream of Hypermethylated CpG Sites in the Hippocampal Dentate Gyrus of Mouse Offspring Developmentally Exposed to HCP

Genome Location	Gene ID	Gene Symbol	Description	Read Counts	
				100 ppm HCP	0 ppm HCP (Control)
Chr 1	MGI: 2443881	*Rasal2*	RAS protein activator like 2	19	3
Chr 2	MGI: 1890647	*Fign*	Fidgetin	26	2
Chr 2	MGI: 2675669	*Nusap1*	Nucleolar and spindle associated protein 1	26	0
Chr 2	MGI: 107464	*Plcb4*	Phospholipase C, beta 4	24	1
Chr 4	MGI: 1921896	*Spsb1*	SplA/ryanodine receptor domain and SOCS box containing 1	19	3
Chr 4	MGI: 1914775	*Trim62*	Tripartite motif-containing 62	24	4
Chr 5	MGI: 2441950	*Adgrl3*	Adhesion G protein-coupled receptor L3	28	3
Chr 7	MGI: 1338823	*Maz*	MYC-associated zinc finger protein (purine-binding transcription factor)	18	3
Chr 7	MGI: 3612342	*Vmn1r90*	Vomeronasal 1 receptor 90	24	2
Chr 8	MGI: 1261835	*Vps37a*	Vacuolar protein sorting 37A	28	5
Chr 10	MGI: 1196373	*Reps1*	RalBP1 associated Eps domain containing protein	26	1
Chr 11	MGI: 94904	*Dlx4*	Distal-less homeobox 4	21	1
Chr 11	MGI: 3044668	*Gsdma3*	Gasdermin A3	22	4
Chr 11	MGI: 96911	*Mafg*	v-Maf musculoaponeurotic fibrosarcoma oncogene family, protein G (avian)	23	4
Chr 11	MGI: 1933227	*Tex14*	Testis expressed gene 14	27	3
Chr 13	MGI: 1923387	*Mcur1*	Mitochondrial calcium uniporter regulator 1	23	2
Chr 17	MGI: 3587025	*Cdkl4*	Cyclin-dependent kinase-like 4	26	4
Chr 19	MGI: 1354733	*Dmrt1*	Doublesex and mab-3 related transcription factor 1	20	0
Chr 19	MGI: 1919449	*Mms19*	MMS19 (MET18 S. cerevisiae)	24	3

Abbreviation: HCP, hexachlorophene.

differences in gene expression between the 0 ppm controls and the 100-ppm HCP-exposed group were calculated using threshold cycle (C_T) values that were first normalized to those of *Hprt* or *Gapdh*, which served as endogenous controls in the same sample, and then relative to a control C_T value using the $2^{-\Delta\Delta C_T}$ method (Livak and Schmittgen, 2001).

Quantitative methylation-specific PCR analysis of candidate genes. Eight genes (*Dlx4*, *Dmrt1*, *Fign*, *Gsdma3*, *Maz*, *Mms19*, *Plcb4*, and *Reps1*) were selected for quantitative methylation-specific PCR analysis with the DNA samples isolated from the 0 ppm controls and the 100-ppm HCP-exposed group on PND 21. The isolated genomic DNA was sonicated using a Bioruptor UCD-250 sonicator (Cosmo Bio Co. Ltd.), mixed with incubation buffer, and then denatured with heat. Twenty percent of the mixture was stored as input DNA at −20°C until use. The remaining mixture was incubated with MBD2/magnetic bead complexes and then eluted. The methylation-enriched DNA was purified using an EpiXplore Methylated DNA Enrichment kit (Clontech Laboratories, Inc.). Input and methylation-enriched DNA samples were used as templates for quantitative measurement of methylation at target CpG sites by real-time PCR using Power SYBR® Green PCR Master Mix (Thermo Fisher Scientific) and a StepOnePlus Real-time PCR System (Thermo Fisher Scientific). The PCR primers for the target gene CpG sites were designed using Methyl Primer Express software Ver. 1.0 (Thermo Fisher Scientific) and Primer Express software Ver. 3.0 (Supplementary Table 2; Thermo Fisher Scientific). The quantification was based on the comparative C_T method and involved a comparison of the C_T values of the methylation-enriched DNA to the C_T values of the input DNA.

Pyrosequencing analysis of candidate genes. The percentages of methylated CpG sites in the target sequences of *Dlx4, Dmrt1, Plcb4*, and *Reps1* were measured with bisulfite-converted DNA using the PyroMark Q24 pyrosequencing system (Qiagen) with the DNA samples isolated from the 0 ppm controls and the 100-ppm HCP-exposed group on PND 21 and PND 77. The isolated genomic DNA was bisulfite converted with an EpiTect® Plus DNA Bisulfite kit (Qiagen) and then used as a template (10 ng) for biotin PCR reactions utilizing a Qiagen PyroMark PCR kit under the following conditions: 95°C for 15 min, (94°C for 30 s, 56°C for 30 s, and 72°C for 30 s) × 45 cycles, and 72°C for 10 min. The sequencing reactions were performed using PyroMark Gold Q24 reagents (Qiagen). Specific pyrosequencing primers were designed to amplify CpG sites using Pyrosequencing Assay Design software Ver. 2.0 (Supplementary Table 3; Qiagen).

Immunohistochemistry. For immunohistochemical analyses, perfusion-fixed brains were additionally fixed by permeation with 4% PFA overnight. Two millimeter coronal slices were prepared at −2.2 mm from bregma in PND 21 offspring brains and at −2.8 mm from bregma in PND 77 offspring brains ($n = 8$–10/group). Brain slices from offspring on PND 21 and PND 77 were further permeation-fixed with 4% PFA overnight at 4°C. Brain slices were processed using a standard protocol for paraffin embedding and were sectioned to a thickness of 3 μm. For immunohistochemistry using "mirror-image" pairs of paraffin sections, the first section of each pair was inverted before floating onto the water bath and picked up on the slide upside-down, and the second section was collected in the conventional manner.

Immunohistochemistry was performed by incubating 3-μm-thick brain tissue sections overnight at 4°C with the antibodies listed in Supplementary Table 4. To quench endogenous peroxidase, the sections were first incubated in 0.3% (v/v) hydrogen peroxide in absolute methanol for 30 min. Immunodetection

was performed using a VECTASTAIN® *Elite* ABC kit (Vector Laboratories Inc., Burlingame, California) with 3, 3′-diaminobenzidine/H_2O_2 as the chromogen. The sections were then counterstained with hematoxylin and coverslipped for microscopic examination.

The following three proteins were selected for evaluation of immunohistochemical distribution after confirming their hypermethylation and transcript downregulation: distal-less homeobox 4 (DLX4), which is encoded by *Dlx4*, doublesex and mab-3-related transcription factor 1 (DMRT1), which is encoded by *Dmrt1*, and phospholipase C beta 4 (PLCB4), which is encoded by *Plcb4*.

For confirming the identity of $DLX4^+$, $DMRT1^+$, and $PLCB4^+$ cells in the dentate hilus as GABAergic interneurons, immunohistochemistry of glutamic acid decarboxylase 67 (GAD67), a GABA-producing enzyme (Houser, 2007), was performed with DLX4, DMRT1, or PLCB4 using mirror sections in a pairwise fashion from an 0 ppm control brain. In addition, immunohistochemistry was performed examining GAD67 and GAD65 for evaluation of any change in the density of GABAergic interneurons between the 0 ppm controls and those exposed to 100 ppm HCP. To examine co-localization of PLCB4 with glutamate metabotropic receptor 1 (GRM1), a glutamate receptor subtype (Maejima *et al.*, 2005), immunohistochemistry was performed examining PLCB4 and GRM1 using serial mirror sections from an 0 ppm control brain. In addition, immunohistochemistry of activity-regulated cytoskeleton (ARC)-associated protein, a member of the immediate-early genes involved in neuronal plasticity (Guzowski, 2002), was performed to investigate the functional relationship of PLCB4 and GRM1.

Morphometry of immunolocalized cells. The $DLX4^+$, $DMRT1^+$, $PLCB4^+$, and $GAD67^+$ cells distributed in the dentate hilus were bilaterally counted in an operator-blinded manner and normalized to the number per unit area of the hilar area (Supplementary Figure 4). ARC^+ cells distributed in the granule cell layer (GCL) were also bilaterally counted in an operator-blinded manner and normalized to the length of the SGZ (Supplementary Figure 4). For quantitative measurement of each immunoreactive cellular component, digital photomicrographs at 400-fold magnification were captured using a BX53 microscope (Olympus Corp., Tokyo, Japan) attached to a DP72 Digital Camera System (Olympus Corp.), and quantitative measurements were performed using the WinROOF image analysis software package (version 5.7, Mitani Corp., Fukui, Japan).

Transcript expression analysis of synaptic plasticity-related genes. To investigate synaptic plasticity changes in the dentate gyrus, transcript levels of synaptic plasticity-related genes, including *Dlg4*, *Gabbr1*, *Gabbr2*, *Gabra1*, *Gabrb2*, *Homer1*, *Stx4a*, and *Syp*, were analyzed by real-time RT-PCR on PND 21 and PND 77 using the PCR primers listed in Supplementary Table 1. *Gabbr1*, *Gabbr2*, *Gabra1*, and *Gabrb2* are GABA receptor family genes and are related to GCL long-term potentiation (Bramham and Sarvey, 1996). *Dlg4* and *Homer1* encode postsynaptic density proteins that play a role in stabilizing expression of the glutamate receptor on the postsynaptic membrane (Kempf *et al.*, 2014; Tu *et al.*, 1999). *Stx4a* and *Syp* encode synaptic vesicle proteins that play a role in synaptic vesicle exocytosis (Mohanasundaram and Shanmugam, 2010; Yong *et al.*, 2013).

Statistical analysis. Numerical data are presented as mean ± SD. Immunoreactive cell counts for each antigen were analyzed using the litter as the experimental unit. Significant differences between the 0 ppm controls and the 100-ppm HCP-exposed group were evaluated as follows. Comparisons of numerical data between 0 ppm controls and 100-ppm HCP-exposed group were made using the *F* test for homogeneity of variance, and Student's *t* test was applied when the variance was homogeneous between the groups as assessed using a test for equal variance. If a significant difference in variance was observed, the Aspin–Welch's *t* test was performed. All analyses were conducted using an Excel Statistics 2010 software package (Social Survey Research Information Co. Ltd., Tokyo, Japan).

RESULTS

In Life Data

With regard to the parameters of dams, no significant difference was observed in reproductive parameters, body weight and food consumption during experiment, and body and brain weights at necropsy on weaning at PND 21 between the 0 ppm controls and 100-ppm HCP-exposed group (Supplementary Tables 5–8; Kato *et al.*, 2016). With regard to the parameters of male offspring, body weight was significantly decreased from PND 13 to PND 21, and brain weight was also significantly decreased on PND 21 in 100-ppm HCP-exposed group compared with 0 ppm controls (Supplementary Tables 9 and 10; Kato *et al.*, 2016).

Hypermethylated Genes Detected by MethylCap-seq Analysis

Nineteen genes with hypermethylated CpG sites located at the promoter region up to 1000 bp upstream from the transcription start site of the gene sequence showed ≥5-fold increase in methylation signals in the 100-ppm HCP-exposed group compared with the 0 ppm controls on PND 21 (Table 1).

Transcript Expression Changes of Candidate Genes in the Dentate Gyrus

Among the 19 genes selected as showing ≥5-fold increase in methylation signals compared with the 0 ppm controls on PND 21, the transcript levels of *Dmrt1, Gsdma3, Mms19*, and *Vmn1r90* were decreased after normalization with *Hprt* and *Gapdh*, and the transcript levels of *Adgrl3*, *Dlx4*, *Fign*, *Maz*, *Plcb4*, and *Reps1* were decreased after normalization with *Hprt* in the 100-ppm HCP-exposed group compared with the 0 ppm controls on PND 21 (Figure 2A). By contrast, no 100-ppm HCP-exposure induced change was detected in transcript levels for *Cdkl4*, *Mafg*, *Mcur1*, *Nusap1*, *Rasal2*, *Spsb1*, *Tex14*, *Trim62*, and *Vps37a* (Supplementary Table 11).

On PND 77, *Dlx4* transcript levels were decreased, whereas *Fign* and *Plcb4* transcript levels were increased in the 100-ppm HCP-exposed group compared with the 0 ppm controls after normalization with *Hprt* and *Gapdh* (Figure 2B). By contrast, no HCP-exposure induced change was detected in transcript levels for *Adgrl3*, *Dmrt1*, *Gsdma3*, *Maz*, *Mms19*, *Reps1*, and *Vmn1r90*.

Validation of Hypermethylation Status by Quantitative Methylation-Specific PCR

The methylation status of *Dlx4*, *Dmrt1*, *Plcb4*, and *Reps1* significantly increased in the 100-ppm HCP-exposed group compared with 0 ppm controls, whereas *Fign*, *Gsdma3*, *Maz*, and *Mms19* displayed no change in methylation status, on PND 21 (Figure 3). Although *Adgrl3* and *Vmn1r90* transcript levels were decreased on PND 21, both genes were excluded from quantitative methylation-specific PCR analysis because we were unable to construct appropriate primers.

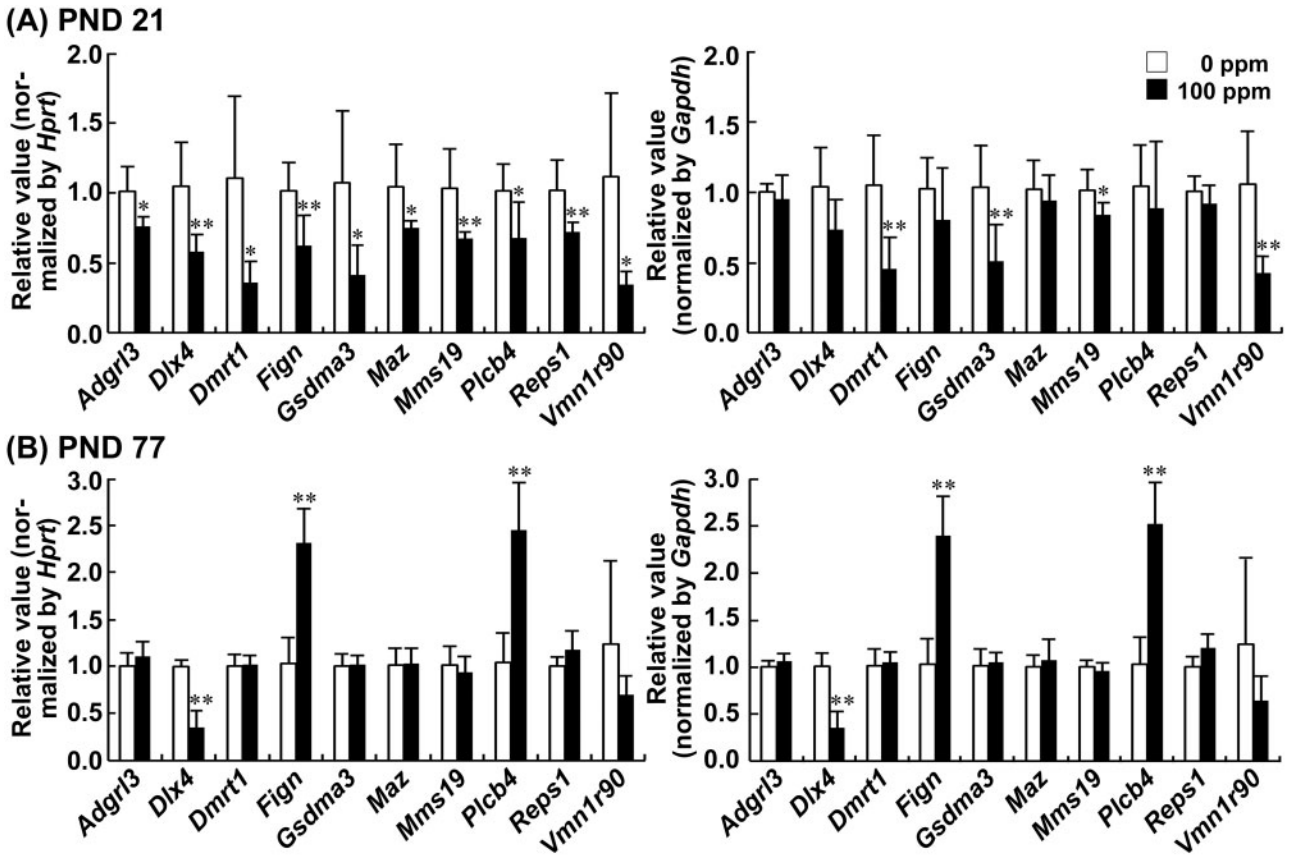

Figure 2. Transcript expression results obtained from MethylCap-seq analysis of hypermethylated genes in the hippocampal dentate gyrus of mice on postnatal day (PND) 21 and PND 77. A, PND 21. B, PND 77. Values are normalized to *Hprt* (left) or *Gapdh* (right) and expressed as the mean + SD; $n = 6$/group. $^{*}p < .05$, $^{**}p < .01$, significantly different from 0 ppm controls by Student's or Aspin-Welch's *t* test.

Evaluation of DNA Methylation Status by Pyrosequencing

In *Dlx4*, *Dmrt1*, *Plcb4*, and *Reps1*, pyrosequencing of nucleotides 368–451, 160–222, 455–524, and 444–500 from the transcription start site, respectively, have CpG sites numbered as 1–16 in *Dlx4*, 1–5 in *Dmrt1*, 1–6 in *Plcb4*, and 1–7 in *Reps1* (Figs. 4 and 5).

On PND 21, cytosine bases in site numbers 1 of *Dlx4*, 3 and 5 of *Dmrt1*, and 3 of *Plcb4* carried greater levels of methylation in the 100-ppm HCP-exposed group than in the 0 ppm controls. Methylation levels of cytosine bases in *Reps1* were unchanged between the two groups.

On PND 77, cytosine bases in site numbers 9 and 16 of *Dlx4*, and 1 and 2 of *Dmrt1* carried greater levels of methylation in the 100-ppm HCP-exposed group than in the 0 ppm controls. Methylation levels of cytosine bases in *Plcb4* and *Reps1* were unchanged between the two groups.

Distribution of Immunolocalized Cells

Using immunohistochemical analysis, we found cells in the hilus of the dentate gyrus expressing protein in their cytoplasm encoded by the hypermethylated genes (i.e., *Dlx4*, *Dmrt1*, and *Plcb4*). Densities of the DLX4^{+}, DMRT1^{+}, and PLCB4^{+} cells in the 100-ppm HCP-exposed group were significantly decreased compared with the 0 ppm controls on PND 21 (Figs. 6A–C). On PND 77, no significant difference was observed in the densities of DLX4^{+}, DMRT1^{+}, and PLCB4^{+} cells between the two groups (Figs. 6A–C; Supplementary Figs. 5A–C).

An analysis of serial mirror sections showed that all subpopulations of cells in the dentate hilus expressing DLX4, DMRT1, or PLCB4 also expressed GAD67 (Figs. 7A–C). The density of GAD67^{+} cells in the dentate hilus was significantly decreased in the 100-ppm HCP-exposed group compared with the 0 ppm controls on PND 21 (Figure 7D). On PND 77, no significant difference was observed in the density of GAD67^{+} cells between the two groups (Supplementary Figure 5D). GAD65 immunoreactivity was only observed in the neuropil, and there were no countable GAD65^{+} cells showing cytoplasmic immunoreactivity in the dentate hilus.

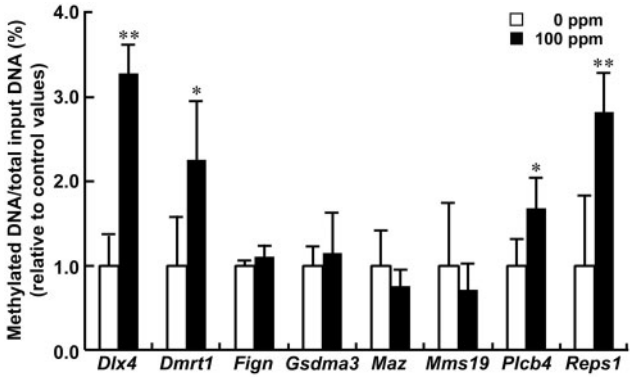

Figure 3. Quantitative methylation-specific PCR data of selected genes in the hippocampal dentate gyrus on postnatal day (PND) 21. Values are expressed as the mean + SD; $n = 5$/group. $^{*}p < .05$, $^{**}p < .01$, significantly different from 0 ppm controls by Student's or Aspin-Welch's *t* test.

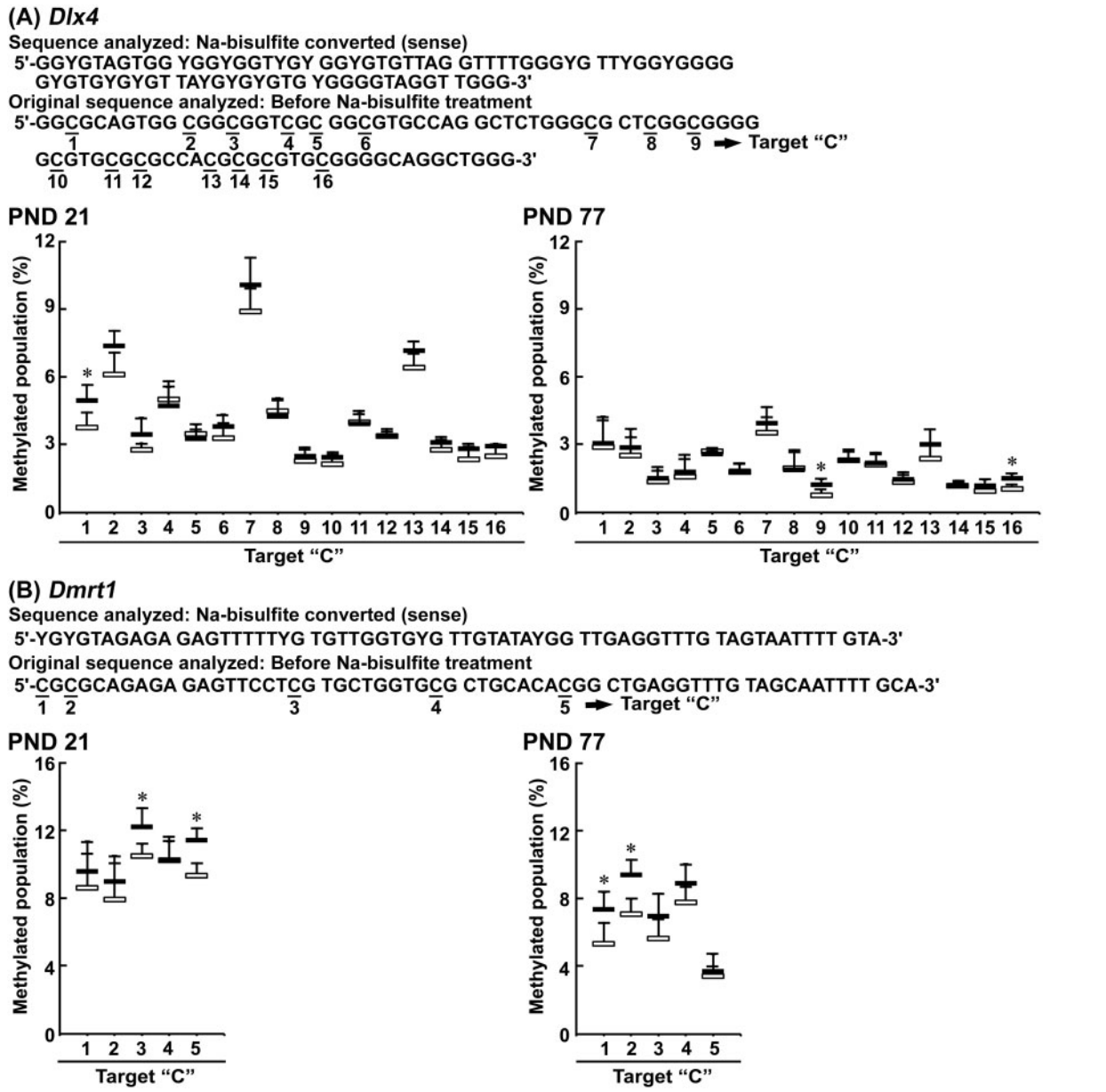

Figure 4. Pyrosequencing results for *Dlx4* and *Dmrt1* in the hippocampal dentate gyrus on postnatal day (PND) 21. A, *Dlx4*. B, *Dmrt1*. All cytosine bases within CpG site are numbered as 1–16 or 1–5. White columns, 0 ppm controls; black columns, 100 ppm hexachlorophene (HCP). Values are expressed as the mean + SD.; $n = 4$/group. $^{*}p < .05$, significantly different from 0 ppm controls by Student's or Aspin-Welch's *t* test.

With regard to PLCB4, an analysis of serial mirror sections showed that the subpopulation of cells in the dentate hilus expressing PLCB4 also expressed GRM1 (Figure 8A). The number of ARC^{+} cells in the GCL was decreased in 100-ppm HCP-exposed group compared the 0 ppm controls on PND 21 (Figure 8B). However, on PND 77, no significant difference was observed in the number of ARC^{+} cells between the two groups (Supplementary Figure 5E).

Transcript Expression Changes of Synaptic Plasticity-Related Genes in the Dentate Gyrus

On PND 21, the transcript level of *Stx4a* was decreased after normalization with *Hprt* and *Gapdh*, and transcript levels of *Dlg4*, *Gabbr1*, and *Gabra1* were decreased after normalization with *Hprt* in the 100-ppm HCP-exposed group compared with the 0 ppm controls (Table 2). By contrast, transcript levels of *Gabbr2*, *Gabrb2*, *Homer1*, and *Syp* did not differ between the two groups. On PND 77, transcript levels of *Gabbr2*, *Gabra1*, and *Gabrb2* were increased, whereas those for *Homer1* and *Stx4a* were decreased after normalization with *Hprt* and *Gapdh* in the 100-ppm HCP-exposed group compared with the 0 ppm controls. Transcript levels of *Dlg4*, *Gabbr1*, and *Syp* did not differ between the two groups.

DISCUSSION

In the present study, we found 19 genes in the hippocampal dentate gyrus of mice exposed to 100 ppm HCP using MethylCap-seq analysis to show hypermethylation of the gene promoter regions up to 1000 bp upstream from the transcription start site sequences. Among them, transcript levels of 10 genes decreased, and 3 of these, *Dlx4*, *Dmrt1*, and *Plcb4*, were confirmed to be hypermethylated by both quantitative

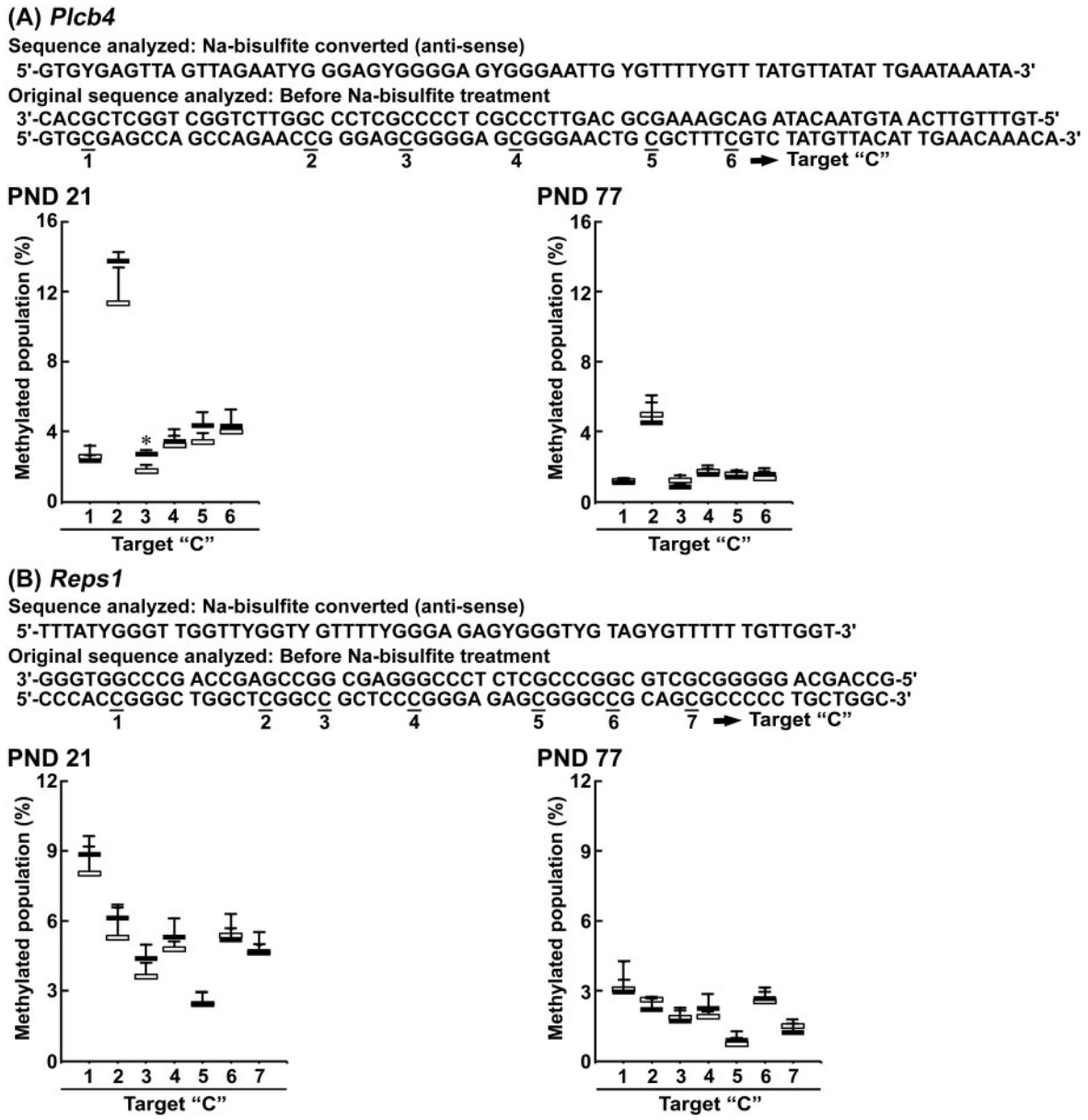

Figure 5. Pyrosequencing results for *Plcb4* and *Reps1* in the hippocampal dentate gyrus on postnatal day (PND) 21. A, *Plcb4*. B, *Reps1*. All cytosine bases within CpG site are numbered as 1–6 or 1–7. White columns, 0 ppm controls; black columns, 100 ppm hexachlorophene (HCP). Values are expressed as the mean + SD; $n = 4$/group. $^{*}p < .05$, significantly different from 0 ppm controls by Student's or Aspin-Welch's *t* test.

methylation-specific PCR and pyrosequencing analyses. Immunohistochemically, the gene products of the three hypermethylated genes DLX4, DMRT1, and PLCB4 were expressed in variable populations of neuron in the dentate hilus and co-expressed GAD67 in variable population in an analysis by mirror section method. It is well-known that not all GABAergic interneurons express GAD67 (Houser, 2007). Therefore, even though not every $DLX4^{+}$, $DMRT1^{+}$, or $PLCB4^{+}$ cells co-expressed GAD67, they are still likely to be GABAergic interneurons. Interestingly, the densities of $DLX4^{+}$, $DMRT1^{+}$, and $PLCB4^{+}$ cells in the dentate hilus were decreased on weaning by developmental HCP exposure, in contrast to the unchanged density of hilar GABAergic interneurons expressing reelin, parvalbumin or calbindin D-28K as demonstrated in our previous study (Kato *et al.*, 2016).

We previously showed that developmental HCP exposure of mice causes myelin vacuolation in the offspring brains (Kato *et al.*, 2016). Although all dentate granule cells have unmyelinated axons (Kress *et al.*, 2008), GABAergic interneurons, as well as other neurons regulating hippocampal neurogenesis from outside the SGZ, have myelinated axons (Jinno *et al.*, 2007). Therefore, developmental HCP exposure may primarily affect the myelin sheath of neurons regulating neurogenesis, including GABAergic interneurons, during development to cause their dysfunction. We have previously discussed the possibility that such HCP-induced myelin vacuolation may reduce the nerve conduction velocity of the cholinergic inputs and GABAergic interneurons (Kato *et al.*, 2016). We also previously found dysfunctional glutamatergic signaling in the dentate gyrus by developmental HCP exposure (Kato *et al.*, 2016). Therefore, the dysfunction of the neurons regulating neurogenesis by developmental HCP exposure in mice may directly or indirectly influence the epigenetic gene expression of *Dlx4*,

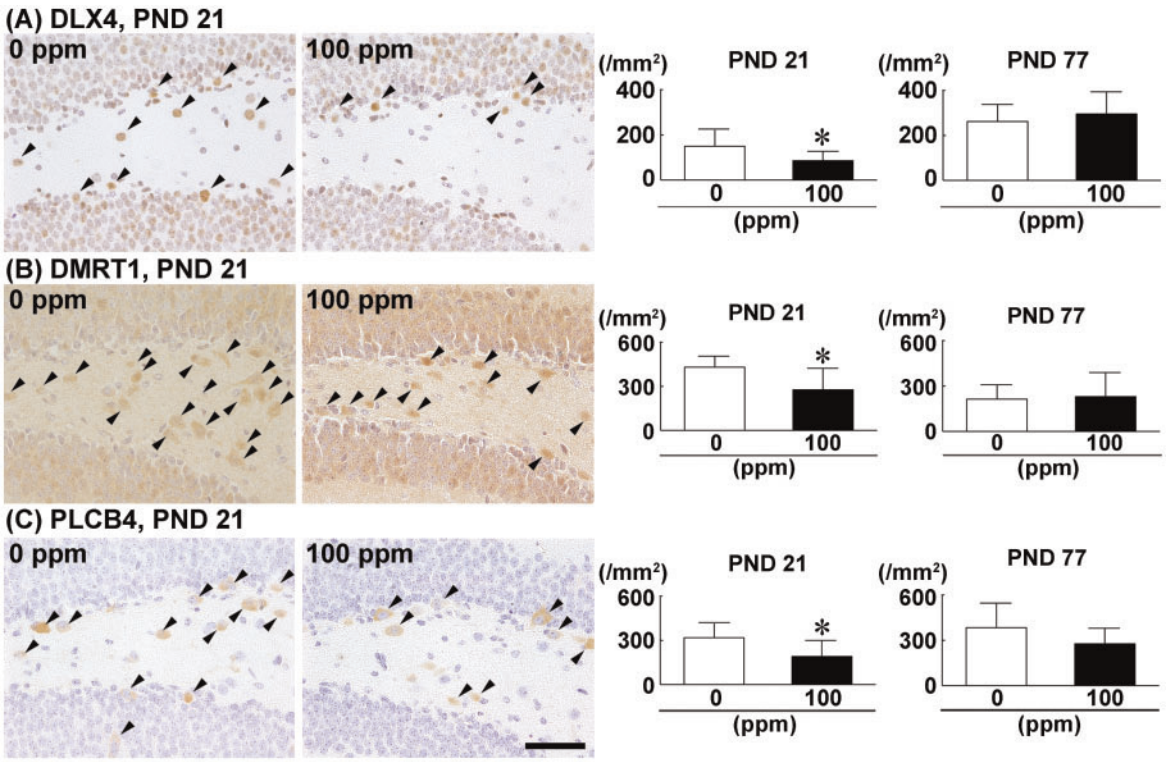

Figure 6. Density of cells immunoreactive for DLX4, DMRT1, and PLCB4 in the hippocampal dentate hilus of male offspring on postnatal day (PND) 21 and PND 77 after maternal exposure to hexachlorophene (HCP) from gestational day 6 to PND 21. A, DLX4. B, DMRT1. C, PLCB4. Representative images from mice exposed to 0 ppm controls (left) and 100 ppm HCP (right) on PND 21. Arrowheads indicate immunoreactive cells. Magnification, ×400; scale bar, 50 μm. Graphs show the density of cells immunoreactive for the indicated molecule in the dentate hilus. $n = 10$/group. $^{*}p < .05$, significantly different from 0 ppm controls by Student's or Aspin-Welch's t test.

Dmrt1, and *Plcb4* in GABAergic interneurons toward downregulation.

Dlx4 is a member of the distal-less homeobox genes (Panganiban and Rubenstein, 2002). *Dlx1/Dlx2* double mutant mice display marked reduction in the numbers of GABAergic interneurons in multiple brain regions (Panganiban and Rubenstein, 2002). This reduction is thought to be due to the lack of the tangential migration of immature GABAergic interneurons from the subcortical telencephalon into the cerebral cortex (Anderson *et al.*, 1997). Therefore, HCP-induced epigenetic downregulation of *Dlx4* observed here may affect the migration of immature GABAergic interneurons to the dentate gyrus. Conversely, it is reported that forced expression of DLX4 in embryonic stem cells induces differentiation to GABAergic neuron-like cells expressing GAD67 (Teratani-Ota *et al.*, 2016). In the present study, developmental HCP exposure induced reduction of $GAD67^{+}$ GABAergic interneurons in the dentate hilus, suggestive of a suppressed differentiation of a progenitor cell population to a GABAergic interneuron subpopulation by epigenetically downregulating *Dlx4*. Because hilar GABAergic interneurons receive cholinergic signals for control of hippocampal neurogenesis (Zhu *et al.*, 2008), the developmental HCP exposure-induced cholinergic receptor downregulation in the dentate gyrus that we have previously shown may be a reflection of reduced GABAergic interneuron subpopulations. Regarding the possibility of the functional involvement of *Dlx* family genes on neurogenesis, *Dlx1/Dlx2* double mutant mice or *Dlx5* or *Dlx6* single mutant mice show aberrant differentiation of progenitor cells in subventricular zone neurogenesis (Panganiban and Rubenstein, 2002). Although the functional involvement of DLX4 on neurogenesis has not been previously shown, there is a possibility that the reduced density of $DLX4^{+}$ GABAergic interneurons suppresses neurogenesis. Importantly, hilar GABAergic interneuron subpopulations regulate proliferation and differentiation of type-2 SGZ progenitor cells (Tozuka *et al.*, 2005). Thus, decline of intermediate progenitor cells by developmental HCP exposure as revealed in our previous study may be caused by the reduction in hilar GABAergic interneurons in relation with the reduction of DLX4.

PLCB4 catalyzes the formation of inositol 1,4,5-trisphosphate and diacylglycerol to function as a second messenger of G protein-coupled receptors, such as the glutamate metabotropic receptor GRM1 (Maejima *et al.*, 2005). We have previously reported that developmental HCP exposure decreases the *Grm1* transcript level in the dentate gyrus in association with disrupted hippocampal neurogenesis (Kato *et al.*, 2016). In the present study, we revealed that a subpopulation of $PLCB4^{+}$ cells was identical to $GRM1^{+}$ cells, and that hilar $PLCB4^{+}$ cells were reduced by developmental HCP exposure. These results suggest that developmental HCP exposure targets the GRM1–PLCB4 signaling cascade in this GABAergic interneuron subpopulation. Pharmacological blockade of perisynaptically distributed GRM1 or GRM5 in interneurons abolishes the long-term potentiation of granule cell mossy fibers through suppression of synaptic plasticity (Hainmüller *et al.*, 2014). In the present study, developmental HCP exposure reduced the number of ARC^{+} cells in the GCL on weaning. ARC is known to play a role in the axonal and synaptic plasticity (Guzowski, 2002). We also demonstrated here the developmental HCP exposure-induced transcript downregulation of the synaptic plasticity-related genes, i.e., *Dlg4*, *Gabbr1*, *Gabra1*, and *Stx4a* (Bramham and Sarvey, 1996; Kempf *et al.*, 2014; Mohanasundaram and Shanmugam, 2010;

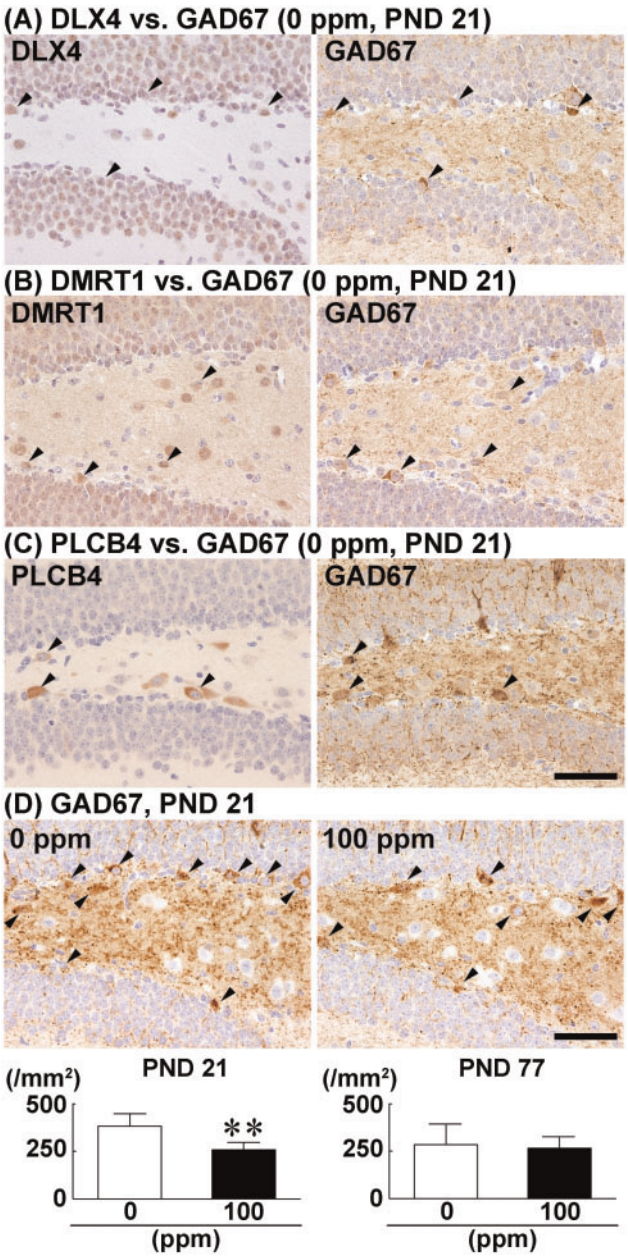

Figure 7. Density of cells immunoreactive for DLX4, DMRT1, and PLCB4 in the dentate hilus in relation to GAD67$^+$ cells. A–C, Cellular identity of DLX4, DMRT1, and PLCB4 with GAD67$^+$ cells analyzed using serial mirror sections. A, DLX4 vs. GAD67. B, DMRT1 vs. GAD67. C, PLCB4 vs. GAD67. Arrowheads indicate cells positive for both GAD67 and the indicated molecule. Magnification, ×400; scale bar, 50 μm. D, Density of GAD67$^+$ cells in the dentate hilus of male offspring on postnatal day (PND) 21 and PND 77 after maternal exposure to hexachlorophene (HCP) from gestational day 6 to PND 21. Representative images from mice exposed to 0 ppm controls (left) and 100 ppm HCP (right) on PND 21. Arrowheads indicate GAD67$^+$ cells. Magnification, ×400; scale bar, 50 μm. Graphs show the density of GAD67$^+$ cells in the dentate hilus. $n = 10$/group. $^{**}p < .01$, significantly different from 0 ppm controls by Student's or Aspin–Welch's t test.

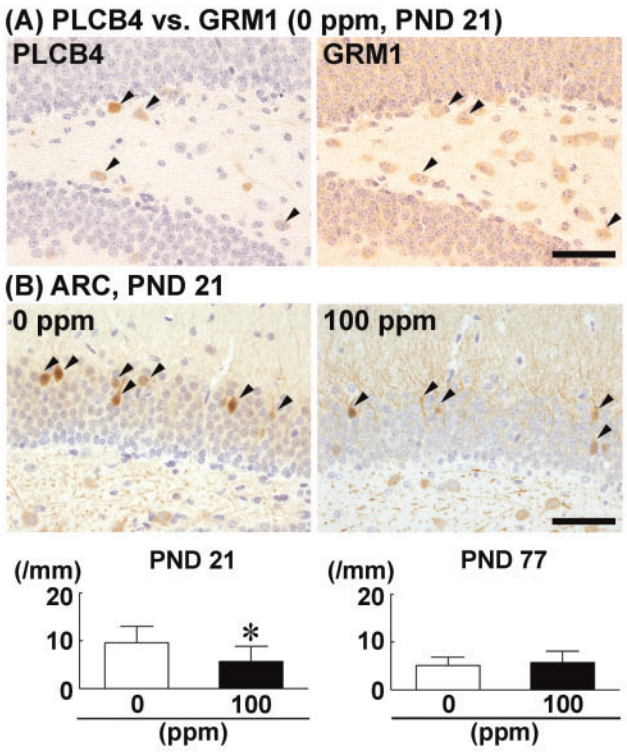

Figure 8. Distribution of GRM1$^+$ cells in the dentate hilus in relation to PLCB4$^+$ cells, and alteration in the number of ARC$^+$ granule cells after maternal exposure to hexachlorophene (HCP). A, Identity of PLCB4$^+$ cells as GRM1$^+$ cells analyzed using serial mirror sections. Arrowheads indicate cells positive for both PLCB4 and GRM1. Magnification, ×400; scale bar, 50 μm. B, Number of ARC$^+$ granule cells in male offspring on postnatal day (PND) 21 and PND 77 after maternal exposure to HCP from gestational day 6 to PND 21. Representative images from mice exposed to 0 ppm controls (left) and 100 ppm HCP (right) on PND 21. Magnification, ×400; scale bar, 50 μm. Graphs show the number of ARC$^+$ cells in the granule cell layer. $n = 8$–10/group. $^*p < .05$, significantly different from 0 ppm controls by Student's or Aspin–Welch's t test.

Tu *et al.*, 1999; Yong *et al.*, 2013), in the dentate gyrus on weaning, suggesting confirmation of suppressed synaptic plasticity on weaning. The transcript downregulation of *Stx4a* was sustained on PND 77, whereas that of *Homer1* first appeared on PND 77, suggestive of sustained suppressed synaptic plasticity until the adult stage. By contrast, transcript upregulation was observed for *Gabbr2*, *Gabra1*, and *Gabrb2* on PND 77, suggestive of an operating compensatory mechanism for suppressed synaptic plasticity. Therefore, it is plausible that developmental HCP exposure causes decreased GCL neuronal plasticity through the reduction of GABAergic interneuron subpopulations active in the GRM1-PLCB4 signaling cascade, and this reduction may involve epigenetic downregulation of *Plcb4* as one mechanism.

DMRT1, a member of a protein family that may share a novel DNA-binding motif called the DM domain, is a transcription factor involved in sexual differentiation, meiosis, and pluripotency in male germline stem cells (Takashima *et al.*, 2013). Overexpression of *Dmrt1* in embryonic stem cells induces differentiation toward neuron-like cells *in vitro* (Yamamizu *et al.*, 2013). However, the role of DMRT1 in neuronal development is not reported. Our current finding that the hilar DMRT1$^+$ cells are GABAergic interneurons suggests an epigenetic downregulation of *Dmrt1* in relation with the suppression of GABAergic interneuron differentiation after developmental HCP exposure.

In the present study, *Dlx4* and *Dmrt1* showed promoter region hypermethylation on PND 77 as well as on PND 21 after developmental HCP exposure; however, the hypermethylated CpG sites differed in both genes between the two time points. Developmental bisphenol A exposure reportedly induces sustained transcript downregulation of *Bdnf* through promoter region hypermethylation in the hippocampus of mouse offspring

Table 2. Transcript Expression of Synaptic Plasticity-Related Genes in the Hippocampal Dentate Gyrus

	0 ppm HCP (Control)		100 ppm HCP	
	Relative Transcript Level Normalized to		Relative Transcript Level Normalized to	
	Gapdh	*Hprt*	*Gapdh*	*Hprt*
No. of Animals Examined	6	6	6	6
PND 21				
Dlg4	1.06±0.39	1.07±0.45	0.79±0.32	0.61±0.22*
Gabbr1	1.05±0.39	1.03±0.29	0.77±0.15	0.65±0.12*
Gabbr2	1.06±0.37	1.06±0.40	0.74±0.18	0.62±0.11
Gabra1	1.03±0.26	1.04±0.30	0.76±0.18	0.64±0.13*
Gabrb2	1.01±0.17	1.02±0.26	1.10±0.31	0.96±0.38
Homer1	1.02±0.20	1.03±0.26	1.30±0.52	1.10±0.61
Stx4a	1.02±0.19	1.03±0.26	0.74±0.14*	0.63±0.12*
Syp	1.02±0.21	1.04±0.35	0.88±0.15	0.75±0.16
PND 77				
Dlg4	1.02±0.22	1.04±0.32	0.92±0.07	0.95±0.14
Gabbr1	1.00±0.08	1.04±0.30	1.13±0.22	1.17±0.21
Gabbr2	1.03±0.23	1.03±0.29	1.53±0.39*	1.59±0.42*
Gabra1	1.02±0.21	1.03±0.26	1.53±0.34*	1.56±0.28**
Gabrb2	1.02±0.21	1.02±0.25	1.53±0.30**	1.58±0.32**
Homer1	1.02±0.21	1.04±0.32	0.52±0.11**	0.54±0.09*
Stx4a	1.03±0.24	1.04±0.28	0.71±0.18*	0.72±0.10*
Syp	1.01±0.17	1.02±0.24	1.16±0.18	1.21±0.21

Data are expressed as the mean ± SD.

Abbreviations: *Dlg4*, discs large MAGUK scaffold protein 4; *Gabbr1*, gamma-aminobutyric acid (GABA) B receptor, 1; *Gabbr2*, gamma-aminobutyric acid (GABA) B receptor, 2; *Gabra1*, gamma-aminobutyric acid (GABA) A receptor, subunit alpha 1; *Gabrb2*, gamma-aminobutyric acid (GABA) A receptor, subunit beta 2; *Gapdh*, glyceraldehyde 3-phosphate dehydrogenase; HCP, hexachlorophene; *Homer1*, homer scaffolding protein 1; *Hprt*, hypoxanthine guanine phosphoribosyl transferase; PND, postnatal day; *Stx4a*, syntaxin 4 A (placental); *Syp*, synaptophysin.

*$p < .05$, and **$p < .01$, significantly different from 0 ppm controls by Student's or Aspin–Welch's *t* test.

until the adult stage, with different CpG sites hypermethylated on weaning and adult stages (Kundakovic *et al.*, 2015). However, transcript downregulation of *Dmrt1* was not sustained on PND 77 in the present study. The previous detection of methylation-sensitive and methylation-insensitive regulatory sequences for transcription in the gene promoter region (Kumar *et al.*, 2016) suggests the hypermethylation at methylation-insensitive CpG sites of *Dmrt1* on PND 77 after developmental HCP exposure. With regard to *Dlx4*, promoter region hypermethylation and transcript downregulation were sustained through PND 77, although these HCP-induced changes were not reflected in the hilar density of the $DLX4^+$ cells. The reason for the unchanged density of $DLX4^+$ cells was unclear, but compensatory mechanisms, such as those involving translational or posttranslational gene control, might have played a role. The epigenetic downregulation of *Plcb4* observed in the present study on weaning was also reversed on PND 77, in parallel with the recovery from aberrant neurogenesis. We have previously shown that a reversibility in hypermethylation and expression downregulation in genes expressed in GABAergic interneurons, in contrast to a sustained downregulation in genes expressed in granule cell lineages, after developmental manganese exposure to cause sustained disruption of hippocampal neurogenesis in mice (Wang *et al.*, 2012, 2013). It may be reasonable to suggest that hypermethylated neural stem cells continue production of hypermethylated granule cell lineage subpopulations to cause sustained hypermethylation through the adult stage. By contrast, methylation in nonproliferative postmitotic GABAergic interneurons may not be increased at the adult stage, and the number of hypermethylated cell populations that can be subjected to removal of excessive methyl bases by demethylation are limited, which differs from granule cell lineages.

In conclusion, our results suggested that the developmental HCP exposure that transiently affected hippocampal neurogenesis caused a transient reduction in GABAergic interneurons expressing DLX4, DMRT1, or PLCB4 in the hilus of the dentate gyrus through epigenetic gene expression downregulation. Developmental HCP exposure also reduced $GAD67^+$ GABAergic interneurons. Considering the role of the *Dlx* gene family in GABAergic interneuron migration and differentiation, the reduction in $DLX4^+$ cells might have decreased the GABAergic interneuron regulating neurogenesis. Developmental HCP exposure also induced influence on granule cell synaptic plasticity to be sustained through the adult stage, and the reduction in GABAergic interneurons active in GRM1–PLCB4 signaling might have been responsible for the suppressed plasticity observed on weaning.

SUPPLEMENTARY DATA

Supplementary data are available at *Toxicological Sciences* online.

ACKNOWLEDGMENT

The authors thank Shigeko Suzuki for her technical assistance in preparing the histological specimens.

FUNDING

Grant-in-Aid for Scientific Research (B) from the Japan Society for the Promotion of Science (JSPS; 25292170); Research Fund from the Institute of Global Innovation Research, Tokyo University of Agriculture and Technology.

REFERENCES

Akane, H., Shiraki, A., Imatanaka, N., Akahori, Y., Itahashi, M., Ohishi, T., Mitsumori, K., and Shibutani, M. (2013a). Glycidol induces axonopathy by adult-stage exposure and aberration of hippocampal neurogenesis affecting late-stage differentiation by developmental exposure in rats. *Toxicol. Sci.* **134**, 140–154.

Akane, H., Saito, F., Yamanaka, H., Shiraki, A., Imatanaka, N., Akahori, Y., Morita, R., Mitsumori, K., and Shibutani, M. (2013b). Methacarn as a whole brain fixative for gene and protein expression analyses of specific brain regions in rats. *J. Toxicol. Sci.* **38**, 431–443.

Anderson, S., Eisenstat, D., Shi, L., and Rubenstein, J. (1997). Interneuron migration from basal forebrain to neocortex: Dependence on *Dlx* genes. *Science* **278**, 474–476.

Bramham, C. R., and Sarvey, J. M. (1996). Endogenous activation of μ and δ-1 opioid receptors is required for long-term potentiation induction in the lateral perforant path: Dependence on GABAergic inhibition. *J. Neurosci.* **16**, 8123–8131.

Cameron, H. A., McEwen, B. S., and Gould, E. (1995). Regulation of adult neurogenesis by excitatory input and NMDA receptor activation in the dentate gyrus. *J. Neurosci.* **15**, 4687–4692.

Ceccatelli, S., Bose, R., Edoff, K., Onishchenko, N., and Spulber, S. (2013). Long-lasting neurotoxic effects of exposure to methylmercury during development. *J. Intern. Med.* **273**, 490–497.

Covic, M., Karaca, E., and Lie, D. C. (2010). Epigenetic regulation of neurogenesis in the adult hippocampus. *Heredity (Edinb.)* **105**, 122–134.

Fonnum, F., Karlsen, R. L., Malthe-Sørenssen, D., Skrede, K. K., and Walaas, I. (1979). Localization of neurotransmitters, particularly glutamate, in hippocampus, septum, nucleus accumbens and superior colliculus. *Prog. Brain Res.* **51**, 167–191.

Guzowski, J. F. (2002). Insights into immediate-early gene function in hippocampal memory consolidation using antisense oligonucleotide and fluorescent imaging approaches. *Hippocampus* **12**, 86–104.

Hainmüller, T., Krieglstein, K., Kulik, A., and Bartos, M. (2014). Joint CP-AMPA and group I mGlu receptor activation is required for synaptic plasticity in dentate gyrus fast-spiking interneurons. *Proc. Natl. Acad. Sci. USA* **111**, 13211–13216.

Houser, C. R. (2007). Interneurons of the dentate gyrus: An overview of cell types, terminal fields and neurochemical identity. *Prog. Brain Res.* **163**, 217–232.

Itahashi, M., Abe, H., Tanaka, T., Mizukami, S., Kimura, M., Yoshida, T., and Shibutani, M. (2015). Maternal exposure to hexachlorophene targets intermediate-stage progenitor cells of the hippocampal neurogenesis in rat offspring via dysfunction of cholinergic inputs by myelin vacuolation. *Toxicology* **328**, 123–134.

Jinno, S., Klausberger, T., Marton, L. F., Dalezios, Y., Roberts, J. D., Fuentealba, P., Bushong, E. A., Henze, D., Buzsáki, G., and Somogyi, P. (2007). Neuronal diversity in GABAergic long-range projections from the hippocampus. *J. Neurosci.* **27**, 8790–8804.

Jones, P. L., Veenstra, G. J., Wade, P. A., Vermaak, D., Kass, S. U., Landsberger, N., Strouboulis, J., and Wolffe, A. P. (1998). Methylated DNA and MeCP2 recruit histone deacetylase to repress transcription. *Nat. Genet.* **19**, 187–191.

Kato, M., Abe, H., Itahashi, M., Kikuchihara, Y., Kimura, M., Mizukami, S., Yoshida, T., and Shibutani, M. (2016). Maternal exposure to hexachlorophene targets intermediate-stage progenitor cells in the hippocampal neurogenesis involving myelin vacuolation of cholinergic and glutamatergic inputs in mice. *J. Appl. Toxicol.* **36**, 211–222.

Kempf, S. J., Casciati, A., Buratovic, S., Janik, D., Toerne, C., Ueffing, M., Neff, F., Moertl, S., Stenerlöw, B., and Saran, A. (2014). The cognitive defects of neonatally irradiated mice are accompanied by changed synaptic plasticity, adult neurogenesis and neuroinflammation. *Mol. Neurodegener* **9**, 57.

Kennedy, G. L., Dressler, I. A., Richter, W. R., Keplinger, M. L., and Calandra, J. C. (1976). Effects of hexachlorophene in the rat and their reversibility. *Toxicol. Appl. Pharmacol.* **35**, 137–145.

Kennedy, G. L., Jr, Dressler, I. A., Keplinger, M. L., and Calandra, J. C. (1977). Placental and milk transfer of hexachlorophene in the rat. *Toxicol. Appl. Pharmacol.* **40**, 571–576.

Kress, G. J., Dowling, M. J., Meeks, J. P., and Mennerick, S. (2008). High threshold, proximal initiation, and slow conduction velocity of action potentials in dentate granule neuron mossy fibers. *J. Neurophysiol.* **100**, 281–291.

Kumar, D. L., Kumar, P. L., and James, P. F. (2016). Methylation-dependent and independent regulatory regions in the Na, K-ATPase alpha4 (*Atp1a4*) gene may impact its testis-specific expression. *Gene* **575**, 339–352.

Kundakovic, M., Gudsnuk, K., Franks, B., Madrid, J., Miller, R. L., Perera, F. P., and Champagne, F. A. (2013). Sex-specific epigenetic disruption and behavioral changes following low-dose in utero bisphenol A exposure. *Proc. Natl. Acad. Sci. USA* **110**, 9956–9961.

Kundakovic, M., Gudsnuk, K., Herbstman, J. B., Tang, D., Perera, F. P., and Champagne, F. A. (2015). DNA methylation of BDNF as a biomarker of early-life adversity. *Proc. Natl. Acad. Sci. USA* **112**, 6807–6813.

Lampert, P., O'Brien, J., and Garrett, R. (1973). Hexachlorophene encephalopathy. *Acta Neuropathol.* **23**, 326–333.

Livak, K. J., and Schmittgen, T. D. (2001). Analysis of relative gene expression data using real-time quantitative PCR and the $2^{-\Delta\Delta C_T}$ method. *Methods* **25**, 402–408.

Maejima, T., Oka, S., Hashimotodani, Y., Ohno-Shosaku, T., Aiba, A., Wu, D., Waku, K., Sugiura, T., and Kano, M. (2005). Synaptically driven endocannabinoid release requires Ca^{2+}-assisted metabotropic glutamate receptor subtype 1 to phospholipase C β4 signaling cascade in the cerebellum. *J. Neurosci.* **25**, 6826–6835.

Masiulis, I., Yun, S., and Eisch, A. J. (2011). The interesting interplay between interneurons and adult hippocampal neurogenesis. *Mol. Neurobiol.* **44**, 287–302.

Maxwell, I. C., and Le Quesne, P. M. (1979). Conduction velocity in hexachlorophene neuropathy: Correlation between electrophysiological and histological findings. *J. Neurol. Sci.* **43**, 95–110.

Mohanasundaram, P., and Shanmugam, M. M. (2010). Role of syntaxin 4 in activity-dependent exocytosis and synaptic plasticity in hippocampal neurons. *Sci. Signal.* **3**, jc7.

Mueller, B. R., and Bale, T. L. (2008). Sex-specific programming of offspring emotionality after stress early in pregnancy. *J. Neurosci.* **28**, 9055–9065.

[OECD] Organisation for Economic Co-operation and Development (2007). Test No. 426: Developmental

Neurotoxicity Study. *OECD Guidelines for the Testing of Chemicals, Section 4*. OECD Publishing, Paris, France.

Panganiban, G., and Rubenstein, J. L. (2002). Developmental functions of the *Distal-less*/Dlx homeobox genes. *Development* **129**, 4371–4386.

Pawluski, J. L., Brummelte, S., Barha, C. K., Crozier, T. M., and Galea, L. A. (2009). Effects of steroid hormones on neurogenesis in the hippocampus of the adult female rodent during the estrous cycle, pregnancy, lactation and aging. *Front. Neuroendocrinol.* **30**, 343–357.

Sun, J., Sun, J., Ming, G. L., and Song, H. (2011). Epigenetic regulation of neurogenesis in the adult mammalian brain. *Eur. J. Neurosci.* **33**, 1087–1093.

Takashima, S., Hirose, M., Ogonuki, N., Ebisuya, M., Inoue, K., Kanatsu-Shinohara, M., Tanaka, T., Nishida, E., Ogura, A., and Shinohara, T. (2013). Regulation of pluripotency in male germline stem cells by Dmrt1. *Genes Dev.* **27**, 1949–1958.

Teratani-Ota, Y., Yamamizu, K., Piao, Y., Sharova, L., Amano, M., Yu, H., Schlessinger, D., Ko, M. S., and Sharov, A. A. (2016). Induction of specific neuron types by overexpression of single transcription factors. *In Vitro Cell Dev. Biol. Anim.* **52**, 961–973.

Tozuka, Y., Fukuda, S., Namba, T., Seki, T., and Hisatsune, T. (2005). GABAergic excitation promotes neuronal differentiation in adult hippocampal progenitor cells. *Neuron* **47**, 803–815.

Tu, J. C., Xiao, B., Naisbitt, S., Yuan, J. P., Petralia, R. S., Brakeman, P., Doan, A., Aakalu, V. K., Lanahan, A. A., Sheng, M., *et al.* (1999). Coupling of mGluR/Homer and PSD-95 complexes by the Shank family of postsynaptic density proteins. *Neuron* **23**, 583–592.

Vivar, C., Potter, M. C., and van Praag, H. (2013). All about running: Synaptic plasticity, growth factors and adult hippocampal neurogenesis. *Curr. Top. Behav. Neurosci.* **15**, 189–210.

Wang, L., Ohishi, T., Shiraki, A., Morita, R., Akane, H., Ikarashi, Y., Mitsumori, K., and Shibutani, M. (2012). Developmental exposure to manganese chloride induces sustained aberration of neurogenesis in the hippocampal dentate gyrus of mice. *Toxicol. Sci.* **127**, 508–521.

Wang, L., Shiraki, A., Itahashi, M., Akane, H., Abe, H., Mitsumori, K., and Shibutani, M. (2013). Aberration in epigenetic gene regulation in hippocampal neurogenesis by developmental exposure to manganese chloride in mice. *Toxicol. Sci.* **136**, 154–165.

Weaver, I. C., Cervoni, N., Champagne, F. A., D'Alessio, A. C., Sharma, S., Seckl, J. R., Dymov, S., Szyf, M., and Meaney, M. J. (2004). Epigenetic programming by maternal behavior. *Nat. Neurosci.* **7**, 847–854.

Yamamizu, K., Piao, Y., Sharov, A. A., Zsiros, V., Yu, H., Nakazawa, K., Schlessinger, D., and Ko, M. S. (2013). Identification of transcription factors for lineage-specific ESC differentiation. *Stem Cell Rep.* **1**, 545–559.

Yong, Z., Yan, L., Dong, Z., Wang, X., Su, R., and Gong, Z. (2013). The effect of chronic thienorphine administration on long-term potentiation and synaptic structure in rat hippocampus. *Synapse* **67**, 779–785.

Zhao, C., Deng, W., and Gage, F. H. (2008). Mechanisms and functional implications of adult neurogenesis. *Cell.* **132**, 645–660.

Zhu, G., Okada, M., Yoshida, S., Ueno, S., Mori, F., Takahara, T., Saito, R., Miura, Y., Kishi, A., Tomiyama, M., *et al.* (2008). Rats harboring S284L *Chrna4* mutation show attenuation of synaptic and extrasynaptic GABAergic transmission and exhibit the nocturnal frontal lobe epilepsy phenotype. *J. Neurosci.* **28**, 12465–12476.